Reconciling age-related changes in behavioural and neural indices of human perceptual decision making

David P. McGovern[1§], Aoife Hayes[1§], Simon P. Kelly[2] & Redmond O'Connell[1]*

[1] Trinity College Institute of Neuroscience and School of Psychology, Trinity College Dublin, College Green, Dublin 2, Ireland
[2] School of Electrical & Electronic Engineering, University College Dublin, Dublin 4, Ireland

[*]Email: mcgoved1@tcd.ie

[§] These authors contributed equally to this work

Abstract

Ageing impacts on decision making behaviour across a wide range of cognitive tasks and scenarios. Computational modeling has proven highly valuable in providing mechanistic interpretations of these age-related differences; however, the extent to which model parameter differences accurately reflect changes to the underlying neural computations has yet to be tested. Here, we measured neural signatures of decision formation as younger and older participants performed motion discrimination and contrast-change detection tasks, and compared the dynamics of these signals to key parameter estimates from fits of a prominent accumulation-to-bound model (drift diffusion) to behavioural data. Our results indicate marked discrepancies between the age-related effects observed in the model output and the neural data. Most notably, while the model predicted a higher decision boundary in older age for both tasks, the neural data indicated no such differences. To reconcile the model and neural findings, we constrained certain model parameters to match our neurophysiological observations. In addition to providing more parsimonious accounts of behaviour on both tasks, the resultant models furnished novel predictions regarding other features of the neural data which were empirically validated. These included a slower mean rate of evidence accumulation amongst older adults during motion discrimination and a beneficial reduction in between-trial variability in accumulation rates in both tasks, which was linked to more consistent attentional engagement. Our findings serve to highlight how combining human brain signal measurements with computational modelling can yield unique insights into group differences in neural mechanisms for decision making.

Key words: Perceptual decision making, ageing, drift diffusion model, neurally-informed modelling, electroencephalography, event-related potential

Introduction

Natural ageing is associated with a progressive decline in many aspects of cognitive function including episodic memory (e.g. Levine et al., 2002), working memory (e.g. Gazzaley et al., 2005), speed of processing (e.g. Salthouse, 1996) and task-switching (e.g. Wasylyshyn et al., 2011). In an effort to better understand these wide-ranging changes, researchers have sought to pinpoint core mental operations that are impacted by ageing (e.g. Salthouse, 1996; Stern, 2002; Park & Reuter-Lorenz, 2009). One such operation is perceptual decision making, the process whereby sensory information is translated into goal-directed actions.

Much of what we know about how ageing affects perceptual decision making comes from behavioural studies employing sequential sampling models (Laming 1968; Link & Heath, 1975; Ratcliff, 1978). The core principle underlying these models is that noisy sensory evidence is accumulated until a predetermined quantity has accrued in favour of one of the decision alternatives. The two most consistent findings to emerge from this work have been an age-dependent widening of decision boundaries (Ratcliff, Thapar, & McKoon, 2001; 2003; 2006a; 2010; Spaniol, Voss & Grady, 2008; Starns & Ratcliff, 2010; Forstmann et al., 2011), consistent with older adults adopting more cautious decision policies (e.g. Rabbit, 1979), and an age-related slowing of non-decision processing indicating a delay in sensory encoding and/or motor execution (Ratcliff, Thapar, & McKoon, 2001; 2003; 2004; 2006a; 2006b; 2007; 2010; Thapar, Ratcliff & McKoon, 2003). Perhaps surprisingly, ageing effects on the parameter that dictates the mean rate of evidence accumulation ('drift rate') vary substantially across studies and appear to be highly task-dependent (e.g. Ratcliff et al., 2001; 2010; 2011, Thapar et al., 2003). For instance, whereas older and younger adults had similar drift rates on a signal detection task (Ratcliff et al., 2001), older adults had slower drift rates on a letter discrimination task (Thapar et al., 2003) and faster drift rates during motion discrimination (Forstmann et al 2011).

While these mathematical models have provided valuable insights into the effects of ageing on decision making, there are limits on what can be gleaned from the modelling of behavioural data alone. For instance, it is difficult to ascertain whether any age-related differences in drift rate emanate from differences in the quality of sensory encoding, the integrity of the evidence accumulation process itself or engagement of other systems that play a supporting role in perceptual decision making, such as neuromodulatory and attention systems which are known to be affected by ageing (e.g. Robertson, 2013). More generally, abstract decision models that quantitatively capture behaviour do not necessarily reflect the neural computations underlying decision formation, as evidenced in recent non-human primate research (Hanks et al 2011; 2014; Heitz and Schall 2013). Some animal

neurophysiology studies have thus begun to use neural signatures of decision formation directly to construct novel model variants that are more representative of the neural implementation of the decision process as well as its behavioural output (Hanks et al., 2014; Purcell & Kiani, 2016). The recent identification of analogous decision signals in non-invasive recordings presents an opportunity to similarly develop neurally-informed models of human decision making. These human brain signals bear all of the same decision-predictive characteristics as have been reported for build-to-threshold decision signals observed in single-unit recordings (e.g. Hanes & Schall, 1996; Roitman & Shadlen, 2002; Ratcliff et al., 2007), including a gradual buildup whose rate predicts reaction time and is proportional to evidence strength, and a fixed amplitude immediately prior to decision reports consistent with a boundary crossing effect (O'Connell, Dockree & Kelly, 2012; Kelly & O'Connell, 2013; De Lange et al., 2013). Two functionally-distinct categories of human decision signals have been characterised: effector-selective signals that represent the translation of sensory evidence into a specific motor plan, such as lateralised oscillatory activity in the beta-band (Donner et al., 2009; O'Connell et al 2012; De Lange et al., 2013; Murphy, Boonstra, & Nieuwenhuis, 2016), and a domain-general signal found in the event-related potential, termed the centroparietal positivity (CPP), that exhibits the same evidence accumulation properties irrespective of whether a response is immediate, delayed (Twomey, Kelly & O'Connell, 2016) or not required at all (O'Connell, Dockree & Kelly, 2012). The buildup of the CPP reliably precedes evidence-selective motor preparation signals (Kelly & O'Connell, 2013), suggesting that it reflects a processing level that intermediates between sensory encoding and motor preparation.

To investigate the impact of ageing on the neural decision process and to examine correspondences with the predictions derived from behavioural modelling, we asked a group of younger and older participants to perform a continuous version of a random dot motion task (Kelly & O'Connell, 2013) and a gradual contrast-change detection task (O'Connell, Dockree & Kelly, 2012), while we recorded 64-channel electroencephalography (EEG). This approach allowed us to isolate both effector-selective and domain-general indices of decision formation whose dynamics we compared to key parameter values derived from fitting the most popular sequential sampling variant, the drift diffusion model (Ratcliff, 1978), to the behavioural data. For the continuous random dot motion task, the diffusion model accounted for age-related performance deficits (longer reaction times and more misses) in terms of a widening of decision boundaries in older adults. However, there were no differences in the amplitude of either the effector-selective or domain-general decision signals at the time of the decision report. Instead, older adults showed slower decision signal buildup of neural evidence accumulation signals, which is equally consistent with the performance deficits. Meanwhile, in the contrast-change detection task, older subjects performed better (less variable reaction times and fewer misses), and while the model

fits explained this by an increase in both drift rate and decision bound, no age-related differences in the corresponding neural signal measurements were observed. We go on to show that if the diffusion model is constrained to take account of these neurophysiological observations, the model provides a comparable fit to behaviour despite having fewer free parameters, as well as producing estimates of the non-constrained parameters that accord with the corresponding neural measures. Specifically, when decision bounds were constrained to be equal in the motion task, the model was then able to capture the drift rate difference evident in the neural data. In the contrast-change task, reduced across-trial variability in drift rate in older adults that became apparent in the neurally-constrained model was reflected in reduced variability both in the buildup rate of the decision signals and in pretarget alpha-band activity, suggesting more consistent attentional engagement. Together, our data suggest that human neurophysiological signals can play an important role in constraining models of perceptual decision making and revealing key mechanistic differences that may go undetected using behavioural modelling alone.

Results

Motion Discrimination

Behaviour

In a first experiment, 35 younger (17 males, age range: 18-38, mean age: 22 years old) and 31 older participants (13 males, age range: 66-83, mean age: 74 years old) performed a continuous version of a random dot motion task in which they were required to discriminate the direction of intermittent periods of coherent motion (randomly set to 30 or 60%) that occurred within a continuous stream of incoherent motion (Figure 1a; Kelly & O'Connell, 2013). For both young and old participants, higher sensory evidence strength (motion coherence) resulted in fewer misses ($p<0.001$ for both age groups, Wilcoxon signed-rank test) and faster reaction times (RTs; $p<0.001$ for both age groups, Wilcoxon signed-rank test). In keeping with previous studies examining the effects of ageing on motion discrimination (e.g. Ball & Sekuler, 1986; Billino, Bremmer & Gegenfurtner, 2008; Forstmann et al., 2011), older adults were significantly less accurate than their younger counterparts for both levels of motion coherence (Figure 1B; 30%: $U=250$, $p<0.001$, 60%: $U=167$, $p<0.001$, Mann-Whitney test) and also displayed significantly slower RTs (Figure 1C; 30%: $U=263$, $p<0.001$, 60%: $U=114$, $p<0.001$, Mann-Whitney test). Further analysis revealed that older adults made more erroneous responses (30% coherence: 2.6% ± 5.4 vs. 0.5 ± 1.2%, $U=357$, $p=0.005$; 60%: 5.4% ± 6.6 vs. 0.8% ± 1.1, $U=199$, $p<0.001$) and more misses (30%: 6.6% ± 10.3 vs. 1.3 % ± 2.1, $U=344$, $p=0.007$; 60%: 0.4% ± 1.1 vs. 0% of targets, $U=473$, $p=0.04$) than their younger counterparts, while

there were no differences in the false alarm rates between the two age groups (Younger (mean±SD): 0.39± 0.5 per block, Older: 0.54 ± 0.7 per block, U=497, p=0.55, Mann-Whitney test).

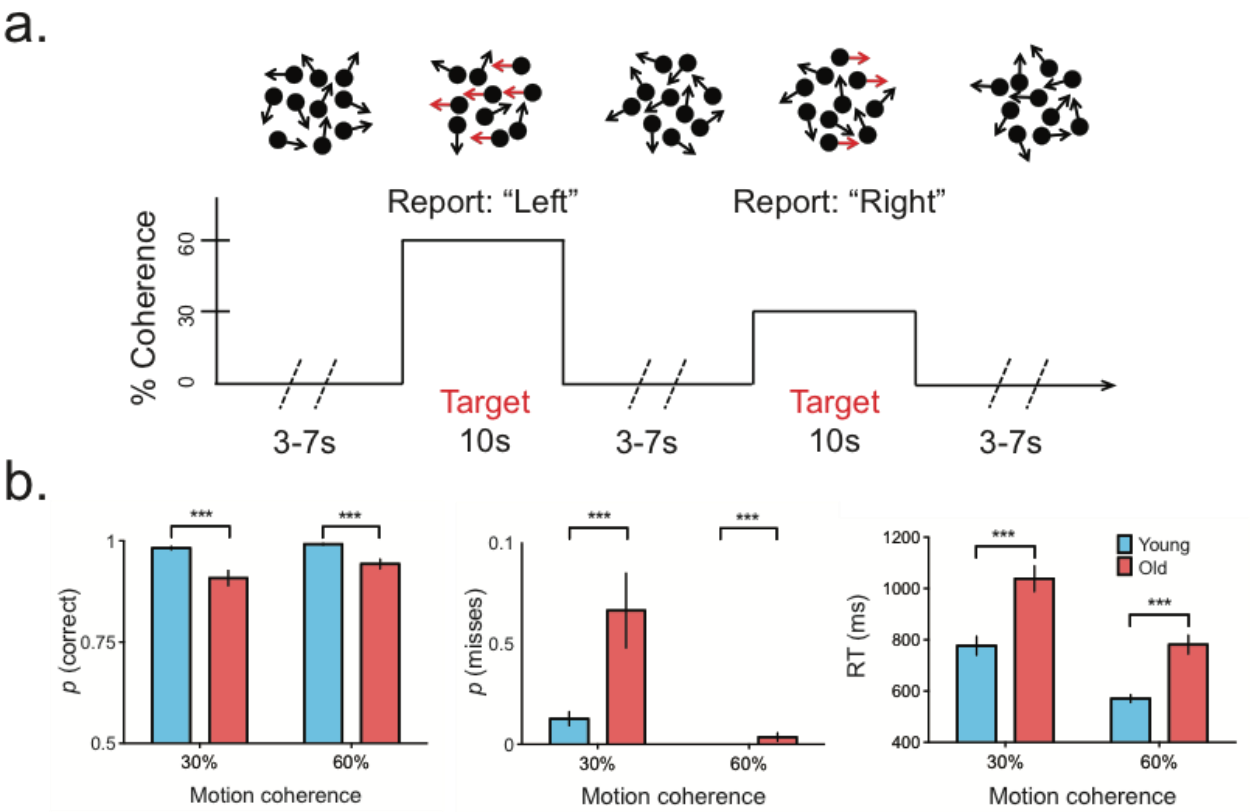

Figure 1: Random dot motion task and associated behaviour. a) Task schematic of the continuous random dot motion task. Participants monitored a centrally-presented dot pattern for transitions from random to coherent motion. b) Older adults were slower and made more incorrect responses at discriminating motion direction than their younger counterparts. Error bars indicate ±1 SEM.

To gain a better understanding of what aspects of the decision process led to these differences in behaviour, we fit a drift diffusion model to the accuracy and RT data for both age groups (Figure 2a). We first identified the key parameters required to fit the model to data pooled across participants from each group (decision bound, drift rate, non-decision time and across-trial drift rate variability, Figure 2b; see *Methods* for further information on our approach), before fitting the model to each individual's data from the two groups (Figure 2c). An analysis of incorrect responses concluded that they are highly unlikely to have arisen from incorrect decision boundary crossings through evidence accumulation (see *Methods* for further details) and therefore incorrect responses were omitted from the fitting procedure. The model produced good fits to the pooled group data for both the younger (G^2= 51.51) and older (G^2= 70.81) groups. Consistent with previous behavioural modelling studies of motion discrimination and other two-alternative perceptual decisions (e.g. Ratcliff,

Thapar & McKoon, 2001; Thapar, Ratcliff & McKoon, 2003; Forstmann et al., 2011), both the group-level and individual fits suggested that older adults had significantly larger boundary separations than younger adults (Figure 2c; U=91, p<0.001, Mann-Whitney test; see also Figure S1a), with no significant differences in drift rate (Figure 3c; *vL*: t(64)=0.23,p=0.82; *vH*: t(64)=0.58, p=0.56). Older adults also had significantly shorter non-decision times (t(64)=2.1, p=0.04).

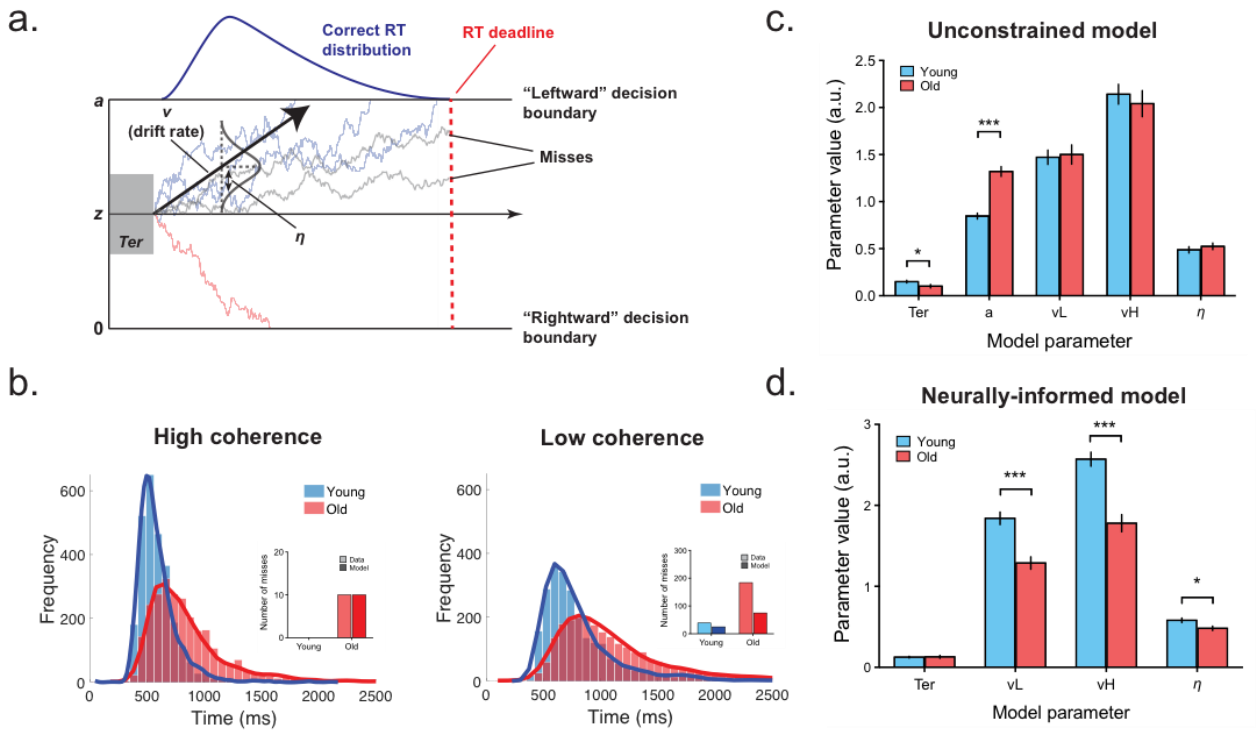

Figure 2: Comparison of diffusion model fits to motion discrimination data with decision boundary free to vary and constrained. a) Schematic of the two-choice drift diffusion model that was fit to the data. Evidence accumulation begins at starting point, *z*, and a response is initiated when the cumulative evidence reaches the correct, *a*, or incorrect, *0*, response boundary. The rate of accumulation is called the drift rate, *v*, which can vary from trial-to-trial. This variability is assumed to be normally distributed with a standard deviation of η. On some trials the cumulative evidence does not reach either decision boundary before the response deadline and in these cases the trial is classified as a miss. b) Neurally-informed model fits (solid lines) to observed reaction time distributions (histograms) pooled across participants. Inset of each panel: Observed and model estimates of target misses. c) Mean parameter estimates derived from model fits to individual data where decision boundary was free to vary. d) Mean parameter estimates derived from model fits to individual data where decision boundary was constrained to be the same across age groups.

Neurophysiology

To measure the impact of ageing on neural evidence accumulation processes, we recorded EEG while participants performed the random dot motion task. In line with our earlier findings (Kelly & O'Connell, 2013; Loughnane et al., 2016), the onset of

coherent motion elicited a rising positivity in the event-related potential over centroparietal scalp regions in both younger and older participants (Figure 3a). However, initial inspection of the data revealed that the buildup of the CPP of the older group actually commenced before the onset of coherent motion suggesting a tendency towards premature evidence accumulation (see Figure S2). To account for this, we baseline-corrected the ERP waveforms of both age groups relative to a 100 ms interval preceding this initial build-up (600 to 500 ms prior to coherent motion; see *Discussion* for further consideration of this analysis step).

Across both groups, the CPP shared many of the key characteristics of the theoretical decision variable central to sequential sampling models, including a gradual buildup whose rate increased in proportion to evidence strength (i.e. motion coherence, $F(1,64)=25.13$, $p<0.001$, $BF_{01}<0.001$), and a stereotyped amplitude immediately prior to response execution that did not differ as a function of coherence ($F(1, 64)= 0.8078$, $p=0.37$, $BF_{01}=3.53$). The rate of CPP buildup differed between the age groups, with a slower rate of accumulation in the older group compared to the young group ($F(1, 64) = 10.73$, $p=0.002$, $BF_{01}=0.005$), while there was no significant difference between age groups in CPP amplitude at response ($F(1, 64) = 1.72$, $p=0.19$, $BF_{01}=1.42$). A qualitatively similar pattern of results was observed at the level of effector-selective motor preparation, with contralateral Mu/Beta activity (Figure 3b) reaching a fixed amplitude before response execution irrespective of evidence strength ($F(1, 64)= 0.61$, $p=0.44$, $BF_{01}=3.9$) or age group ($F(1,64)=2.76$, $p=0.1$, $BF_{01}=1.84$). Also in keeping with the CPP results, the buildup rate of contralateral Mu/Beta was faster for higher motion coherence ($F(1,64)=10.85$, $p=0.002$, $BF_{01}=0.007$) and in younger adults ($F(1,64)=5.9$, $p=0.018$, $BF_{01}=0.34$).

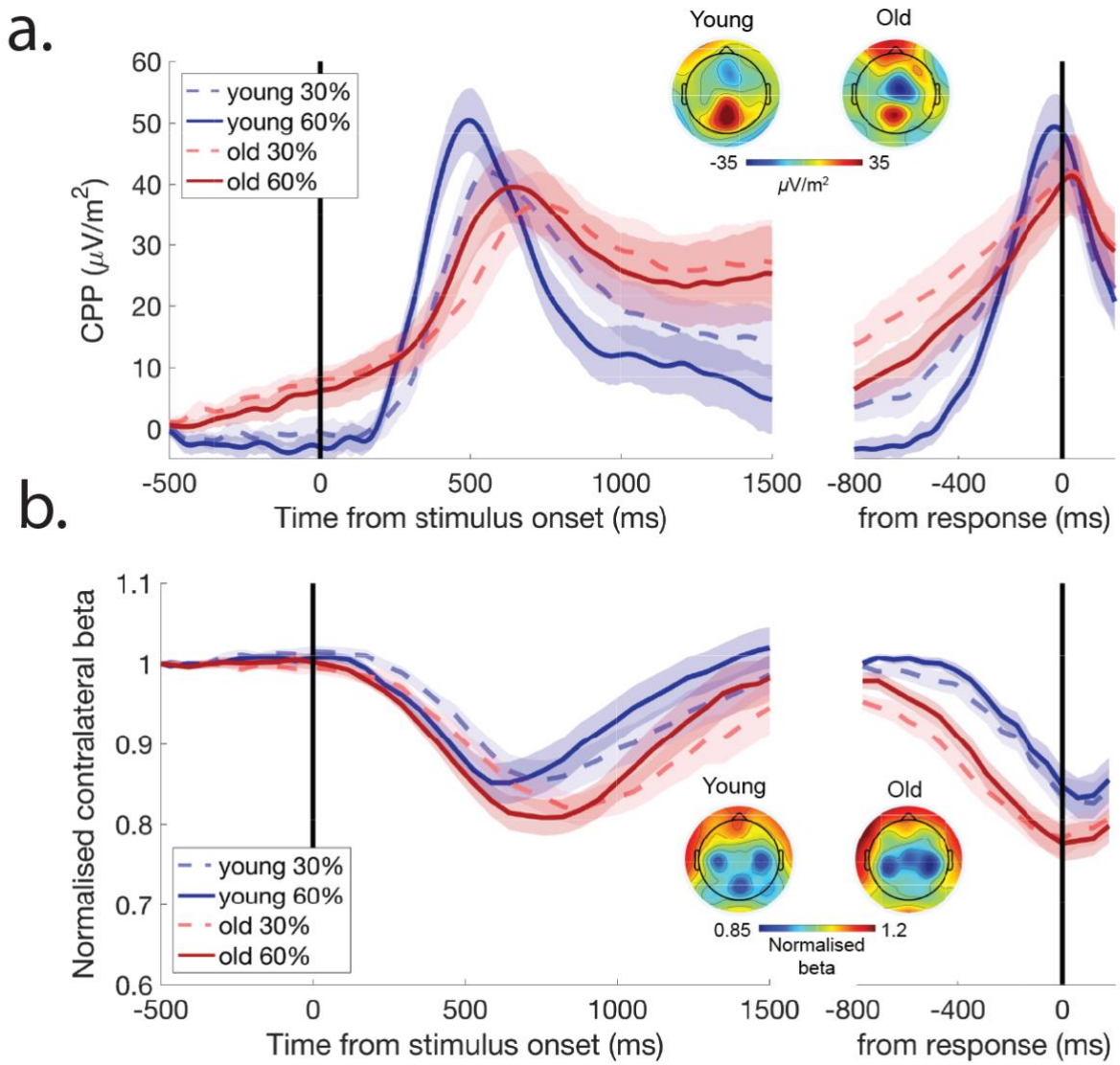

Figure 3: During motion discrimination older adults exhibit a slower rate of evidence accumulation relative to younger adults, with both age groups displaying similar amplitudes at response. a) Stimulus-locked (left) and response-locked (right) CPP waveforms for young and older participants performing the continuous random dot motion task. The rate of CPP buildup differed between the age groups, with a slower rate of accumulation in the older group compared to the young group, while there was no difference in CPP amplitude between the different age groups at the time of decision report (black solid line on right panel). b) A similar pattern of results was observed for contralateral Mu/Beta activity. Shaded areas indicate ±1 SEM of data points.

Neurally-informed modelling

Our neurophysiological data indicate that age-related decrements in motion discrimination performance arise due to slower accumulation of motion information in older adults, with little or no difference in the decision boundary positions of younger and older participants. However, these observations are at odds with our

behavioural modelling results and those of previous studies (e.g. Forstmann et al., 2011). In an effort to address this discrepancy, we fit an additional model to the behavioral data in which, based on our neurophysiological observations, the decision bound was fixed to the mean of the young and older group parameter values from the original group-level model fits (see *Methods*). The model fits from this neurally-constrained model were comparable to the unconstrained model for both the younger (G^2= 58.37) and older (G^2= 74.13) groups. Moreover, the age group differences in the unconstrained parameter values from this model were more in keeping with our neurophysiological data, with significantly lower drift rate in older subjects for both low and high coherence stimuli (Figure 3d; *vL*: U=220, p<0.001, *vH*: U=182, p=0.001, Mann-Whitney tests; see also Figure S1b). Between-trial drift rate variability was also significantly higher in younger participants than older participants (t(64)=2.6, p=0.013; see *Contrast-change detection task* for further analysis and discussion).

To determine the impact of fixing the decision boundary on the model's ability to account for the behavioural data, we calculated Bayesian Information Criterion (BIC) values for the fits of the original (5 free parameters) and neurally-informed (4 free parameters) models to the group-level data. This analysis indicated that the neurally-informed model (Younger: 93.29, Older: 108.37) outperformed the original model (Younger: 95.17, Older: 113.69) for both younger and older participants). Thus, fixing the decision boundary resulted in a model that provided a more parsimonious account of the behavioural data while also showing an age-related decrease in drift rate consistent with the observation of slower decision signal build-up rates.

Contrast-change Detection

Behaviour

To assess whether the age-related effects we observed on the random dot motion task generalised to other perceptual decision making tasks, the same participants performed a contrast-change detection task (O'Connell, Dockree & Kelly, 2012) within the same testing session, with the order of the tasks counterbalanced across participants. Participants were required to continuously monitor a checkerboard stimulus for intermittent reductions in contrast, which were reported via a right hand button click (Figure 4a). Older adults surprisingly outperformed their younger counterparts on this task, detecting more of the contrast reductions (Figure 4b; U=456, p=0.005, Mann-Whitney test) despite maintaining similar average response times (Figure 4c; t(74)=0.179, p=0.86) and false alarm rates (Younger: 1.6 per block ± 1.4, Older: 1.6 per block ± 1.9, U=636, p=0.37, Mann-Whitney Test). The younger group did, however, display increased RT variability compared to the older group

(Mean coefficient of variation across participants: Younger= 0.234, Older=0.209, t(74)=2.5, p=0.015). A one-choice drift diffusion model (Figure 5a; Ratcliff & Van Dongen, 2011), with the same free parameters as in the analysis of the motion discrimination (decision bound, drift rate, non-decision time, between-trial drift variability), provided a good fit to the pooled group data (Figure 5b) for both the younger (G^2=84.24) and older (G^2=87.33) groups. The parameter estimates from the fits of this model to the individual data indicated that the behavioural advantage in the older group was linked to the combined effect of two distinct parameter differences: higher drift rates (Figure 5c; t(74)=3.26, p=0.002; see also Figure S3a), as well as wider decision boundary separations than young adults (t(74)=2.4, p=0.02).

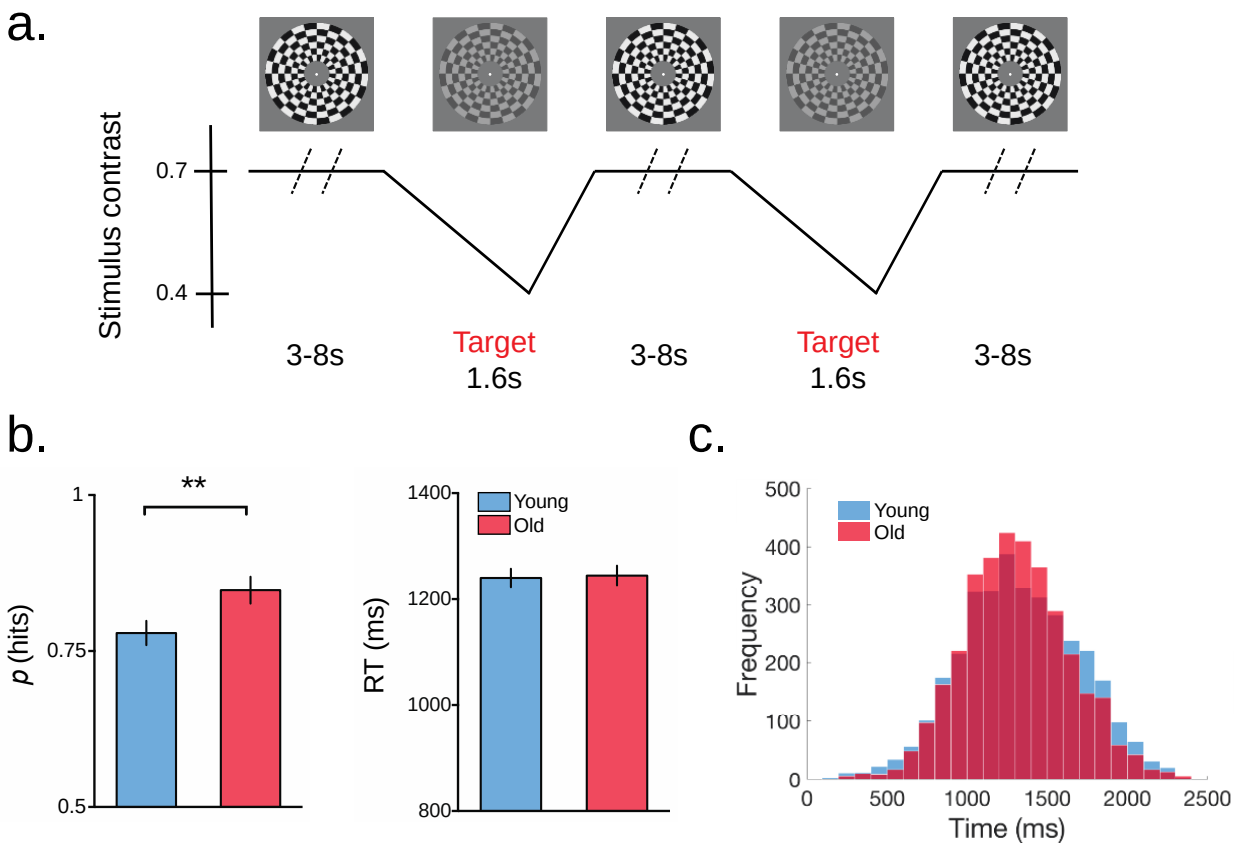

Figure 4: Gradual contrast-change detection task and associated behaviour: a) Schematic of contrast-change detection task. Participants monitored a checkerboard annulus for intermittent decreases in stimulus contrast. b) Older adults detected more of the contrast targets than younger adults, while maintaining similar reaction times. c) Reaction time distributions for young and older age groups.

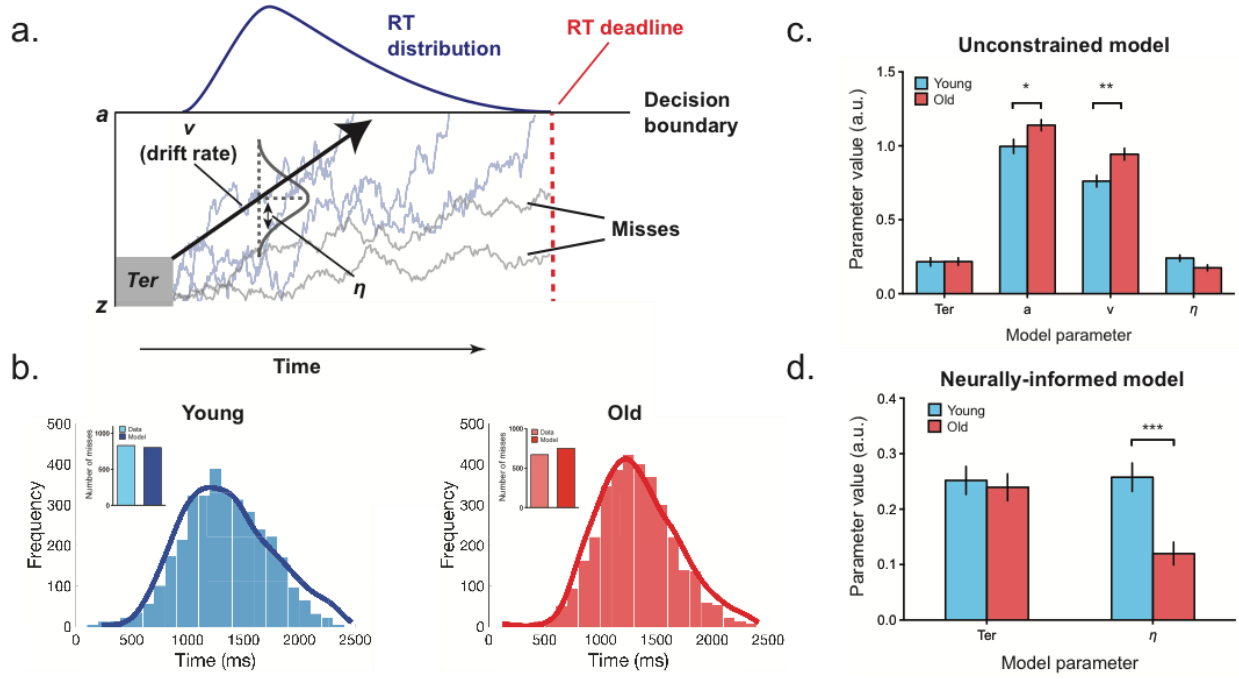

Figure 5: Comparison of diffusion model fits to contrast-change detection data with decision boundary and drift rate free to vary and constrained. a) Schematic of the one-choice drift diffusion model that was fit to the data. Evidence accumulation begins at starting point, *z*, and a response is initiated when the cumulative evidence reaches the decision boundary, *a*. The rate of accumulation is called the drift rate, *v*, which can vary from trial-to-trial. This variability is assumed to be normally distribution with a standard deviation of η. On some trials the cumulative evidence does not reach the decision boundary before the response deadline and in these cases the trial is classified as a miss. b) Neurally-informed model fits (solid lines) to observed reaction time distributions (histograms) pooled across participants. Inset of each panel: Observed and model estimates of target misses. c) Mean parameter estimates derived from model fits to individual data where decision boundary and drift rate were free to vary. d) Mean parameter estimates derived from model fits to individual data where decision boundary and drift rate were constrained.

Neurophysiology

To examine whether comparable effects were observed in the neural indices of decision formation, we again measured the CPP and left hemisphere beta (LHB) as assays of sensory evidence accumulation and motor preparation, respectively. In addition to these measures, the gradual contrast detection task also allowed us to track the basic sensory encoding of contrast over time by measuring the amplitude of the occipital steady-state visual evoked potential (SSVEP; Di Russo et al., 2007; O'Connell et al 2012) generated by the on-off flicker of the checkerboard stimulus. Although the amplitude of the SSVEP was greatly reduced in the older group compared to the young group, when the signals were normalised to take account of these baseline differences (see *Methods* for further details), the SSVEPs for both age groups reliably tracked the decrease in stimulus contrast displaying remarkably

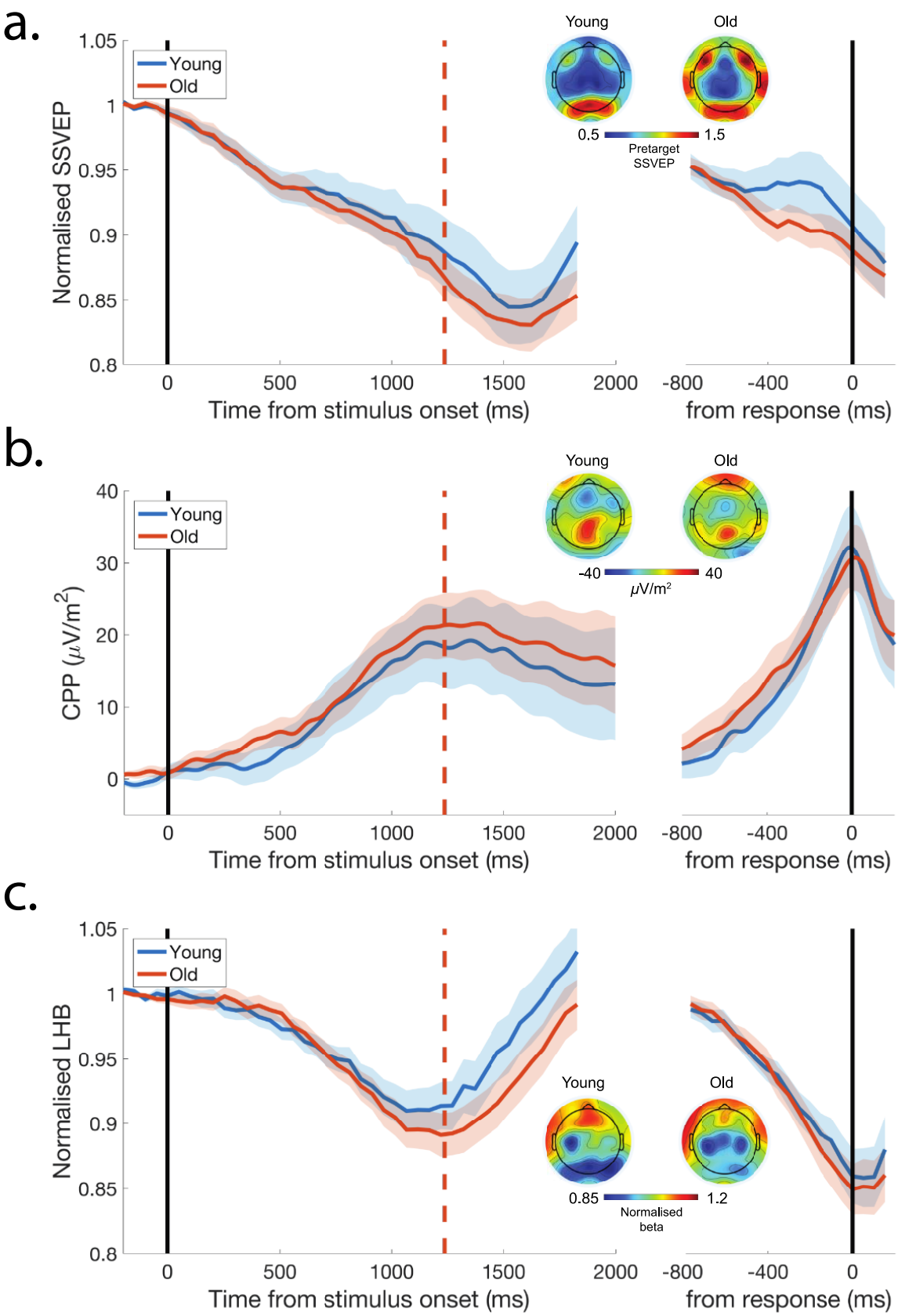
a.
Young
Old
Normalised SSVEP
1.05
1
0.95
0.9
0.85
0.8
0
500
1000
1500
2000
Time from stimulus onset (ms)
-800
-400
0
from response (ms)
Young
Old
0.5
1.5
Pretarget SSVEP
b.
Young
Old
CPP (μV/m^2)
40
30
20
10
0
0
500
1000
1500
2000
Time from stimulus onset (ms)
-800
-400
0
from response (ms)
Young
Old
-40
40
μV/m^2
c.
Young
Old
Normalised LHB
1.05
1
0.95
0.9
0.85
0.8
0
500
1000
1500
2000
Time from stimulus onset (ms)
-800
-400
0
from response (ms)
Young
Old
0.85
1.2
Normalised beta

348

Figure 6: Sensory encoding, decision formation and motor preparation signals exhibit similar dynamics in young and older participants on the contrast-change detection task. a) Stimulus-locked (left) and response-locked (right) SSVEP displays similar buildup rates and amplitudes at response for both age groups. A similar pattern was observed for both the CPP (b) and for left hemisphere beta (LHB) band activity (c). Dashed lines on stimulus-locked CPP and LHB indicate mean reaction times of both age groups.

similar stimulus- and response-aligned waveforms (Figure 6a). Furthermore, both the CPP (Figure 6b) and LHB (Figure 6c) were very similar across age groups, with no significant differences in the buildup rates (CPP: $t(74)=1.18$, $p=0.24$, $BF_{01}=3.02$; LHB: $t(74)=0.99$, $p=0.32$, $BF_{01}=3.64$) or peak amplitudes (CPP: $t(74)=0.68$, $p=0.5$, $BF_{01}=4.62$; LHB: $t(74)=0.16$, $p=0.88$, $BF_{01}=5.66$) of these signals in the response-aligned waveforms.

Neurally-informed modelling

Our initial neural signals analysis did not uncover any differences at the sensory encoding, decision formation or motor preparation processing levels that could account for the enhanced contrast detection performance of the older participants. As in the random dot motion data, these electrophysiological data appear to be at odds with our findings from a fit of a standard model, which suggested that older adults displayed higher rates of evidence accumulation and elevated decision boundaries. In an attempt to reconcile these findings, we fixed the boundary criterion and drift rate parameters to intermediate values between the younger and older values derived from the initial model fit (4 free parameters) and fit the resulting model (2 free parameters) to the behavioural data (Figure 5b). While the fits of this reduced model to the pooled data were marginally worse compared to the unconstrained model fits for both younger ($G^2=97.31$) and older ($G^2=90.72$) groups, the BIC values indicated that the constrained model (Younger: 113.79, Older: 107.2) provided a more parsimonious fit to the data compared to the original model (Younger: 117.19, Older: 120.3) with 4 free parameters. Fitting this neurally-constrained model to the individual data suggested that the key factor underlying the age-related behavioural advantage was a higher degree of between-trial drift rate variability in younger adults compared to older adults (Figure 5d; $U=359$, $p<0.001$, Mann-Whitney test). In the following section we sought evidence in our neurophysiological data to support these model findings.

Linking neurally-informed modelling to neurophysiology

The results from the neurally-constrained diffusion model suggest that the main factor driving the older adults' behavioural advantage on the contrast-change detection task is reduced between-trial drift rate variability. To establish whether there was a corresponding age-related reduction in the variability of the neural

signatures of decision formation, we calculated single-trial estimates of the CPP slope for the two age groups. This analysis revealed that the buildup rate of the CPP was significantly more variable in the young group compared to the older group (Mean SD across participants: Young=0.31, Old=0.21, $t(74)=5.7$, $p<0.001$) in keeping with the modelling results. Furthermore, a similar age-related reduction in the variability of the buildup rate of the CPP was also observed in the data from the random dot motion task (Median SD across participants: Young=0.16, Old=0.13, $U=385$, $p=0.04$, Mann-Whitney Test) suggesting that this effect generalises across different perceptual tasks.

One potential reason for the age-dependent decrease in between-trial variability of evidence accumulation is that older adults maintained a greater level of engagement with the task (e.g. Forstmann et al., 2011), while younger participants may have been more susceptible to fluctuations of attention over the course of the experiment. Although the current experiment did not directly manipulate the effect of attention on task performance, the amplitude of alpha-band activity over posterior scalp sites is a well-known electrophysiological signature of endogenous attention (e.g. Hanslmayr et al., 2007; O'Connell et al., 2009; Kelly & O'Connell, 2013). In line with the idea that younger adults may be more susceptible to fluctuations of attention, across-trial variability of alpha band activity (coefficient of variation, CV) was higher for younger participants compared to their older counterparts (Young: 0.231, Old: 0.185, $t(74)=3.14$, $p=0.002$).

Discussion

Our results highlight ways in which human brain recordings and abstract computational models can be used to reciprocally inform one another to gain deeper insights into the factors that shape perceptual decision making. For both motion discrimination and contrast-change detection decisions, the initial behavioural modelling and neural signal measurements pointed to very different explanations for age-related changes in decision making performance. However, fixing certain model parameters whose corresponding neural measurements did not differ between the two groups (i.e. bound for motion discrimination, bound and drift rate for contrast-change detection), produced estimates of the remaining unconstrained parameters that could account for the observed ageing effects on the neural decision signals as well as behaviour. Furthermore, the neurally-constrained model fits uncovered additional, novel effects which were in turn confirmed in follow-up neural signal analysis.

Like many other studies to examine the effects of ageing using sequential sampling models (e.g. Ratcliff, Thapar & McKoon, 2001; 2006b; 2007; Starns & Ratcliff,

2010; Forstmann et al., 2011), our initial model fits to the behavioural data suggested that the main age-related adjustment in decision making was a widening of the decision boundaries. However, these modelling results ran contrary to our neural signals analysis, which showed no significant age-related differences in the amplitude of either the domain-general or effector-selective signatures of evidence accumulation at the time of decision report. These neurophysiological observations suggest that, in the current experiments, younger and older adults applied similar decision policies. This is not to say that older adults do not exhibit enhanced response caution in some situations. The requirement to continuously monitor stimuli for temporally unpredictable feature changes renders our tasks qualitatively different to those used in previous work in which trials are discretely presented and the stimulus onset provides a cue for the initiation of evidence accumulation (e.g. Forstmann et al., 2011). Here, the unpredictable evidence onsets and instructions to respond only when sure likely encouraged the implementation of conservative decision policies in both groups. It may be that older adults do exhibit relatively higher decision boundaries when placed under greater time pressure but our results highlight that any such differences do not generalise to all scenarios.

A further advantage of this modelling approach is that it generated novel predictions regarding the neural data which would otherwise have been overlooked. Our initial analysis of the sensory encoding and decision signals elicited during the contrast-change detection task provided no clear explanation as to why the older adults performed better than younger adults. While the initial model fits to the behavioural data indicated significant age group differences in both drift rate and boundary separation, we did not observe any differences in the corresponding neural measurements (decision signal build-up rates and amplitudes at response, respectively). When the model was constrained to match these neural observations, it accounted for the poorer performance of younger adults via increased trial-to-trial variability in drift rate. Thus, the neurally-constrained model yielded a new, empirically testable prediction that young participants should exhibit greater trial-to-trial variability in the build-up rate of the CPP and, indeed, we found this to be the case during both the contrast and motion discrimination tasks. The increased variability of drift rates and more variable decision signal build-up of the young group were also accompanied by increased variability in posterior alpha-band activity, an established oscillatory marker of attentional engagement (e.g. Hanslmayr et al., 2007; O'Connell et al 2009; Dockree et al 2017). These results suggest that older participants were able to maintain attentional engagement more consistently across the duration of the tasks. It cannot be determined here whether this effect reflects a compensatory strategy on the part of the older group or increased motivation to perform well on the task. Regardless, these results serve to highlight how combining neurophysiological data with behavioural modelling make it possible to disentangle positive and negative aging effects.

Whereas older adults displayed smaller drift rate parameter estimates coupled with slower mean buildup rates of the abstract and effector-selective decision signals on the random dot motion task, no such effects were observed on the contrast-change task. Thus, age-related drift rate reductions are likely due to task-specific deficits in sensory encoding affecting the quality of evidence entering the decision process. These findings are in keeping with the literature on the effects of age on sensory processing; while there is ample psychophysical (Ball & Sekuler, 1986; Betts et al., 2005; Bennett, Sekuler & Sekuler, 2007) and neurophysiological (Yang et al., 2008; Yang et al., 2009; Liang et al., 2010) evidence to suggest that motion processing declines with increasing age, sensitivity to stimuli of relatively low spatial frequency and high contrast, such as the checkerboard stimuli used in the current study, appears to be preserved in older adults (Owsley, Sekuler & Siemsen, 1983; Elliott, Whitaker & MacVeigh, 1990; Habak & Faubert, 2000). Thus, taken together, our neurophysiological data suggest that ageing does not lead to a fundamental decline in perceptual decision formation processes per se, but rather impacts on certain sensory inputs. An implication of these observations is that remediation strategies aimed at enhancing perceptual decisions in older adults should target those specific aspects of sensory processing that are subject to age-related decline.

One aspect of the neural data that is not readily accounted for in the standard drift diffusion model was the early build-up of the CPP in older adults on the random dot motion task. The reasons for this early buildup are unclear. One possibility is that older participants implemented a different evidence accumulation strategy in comparison to the younger group. The early CPP buildup could, for example, reflect a tendency to accumulate throughout the inter-target interval in order to ensure that no evidence will be missed once it appears. While the models implemented in this study provided a parsimonious account of the behavioural data and key elements of the neurophysiological data, it is likely that additional algorithmic elements are necessary to provide a more complete account of the neural implementation. These are important considerations for future work.

Leveraging human brain signatures of decision formation to constrain computational signals has potential benefits that extend beyond research on ageing. Recent studies have suggested that the full drift diffusion model may be more complex than required in certain circumstances and this complexity can lead to more variable parameter estimates (Lerche & Voss, 2016; 2017; van Ravenzwaaij, Donkin & Vandekerckhove, 2017). The key message from these studies is that the sensitivity of diffusion models to between-group effects can be enhanced by reducing or constraining some of its parameters. However, determining which parameters should be constrained in a given experiment is not straightforward. For example, the EZ diffusion model (Wagenmakers, van der Maas & Grasman, 2007) does not include

between-trial variability in any of its parameters and has been shown to be a more powerful tool at detecting simulated between-group effects as a result of this simplification (van Ravenzwaaij, Donkin & Vandekerckhove, 2017). Yet, our neurophysiological data suggest that its exclusion in the present context would overlook an important aspect of how ageing impacts the decision-making process. Here, we show that inspection of neurophysiological signals reflecting decision formation processes can provide a principled way of constraining the parameters of abstract decision models (see Hanks et al., 2014; Murphy et al., 2016; Purcell & Kiani, 2016 for similar approaches). Given the success of this approach in reconciling the differences in our behavioural and neural indices of decision making, this study paves the way for using similar techniques to address questions in clinically-relevant groups with impaired decision making, such as those with ADHD (e.g. Hauser et al., 2016) and those suffering from addiction (e.g. Bechara, 2005).

Methods

Participants

Thirty-nine younger and 42 older adults volunteered to take part in the study. The younger participants were recruited from the student population of Trinity College Dublin and compensated with research credits for their time, while older participants were recruited from the Trinity College Institute of Neuroscience volunteer participant panel. Criteria for inclusion in the study were right-handedness; normal or corrected-to-normal vision; no personal history of neurological or psychiatric illness, brain injury, abuse of substances or use of psychotropic drugs; no personal history or family history of epilepsy, unexplained fainting or sensitivity to flickering light; and a minimum score of 26 on the Mini Mental State Examination (MMSE). The age groups were matched for gender and years of education (Younger: 15.1, Older: 15.9), however, the younger group had a significantly higher average score on the MMSE than the older group (Young: 28.8, Older: 27.7, $p<0.001$). All participants were naive to the purposes of the study and provided written consent to participate. Participants were excluded if more than two-thirds of their trials were rejected due to EEG artifacts. This led to the rejection of two young participants and four older participants on the random dot motion task and one young participant and four older participants on the contrast-change detection task. A further two young and seven older participants were excluded from the random dot motion task due to technical issues during data acquisition. Following participant rejection for each experiment, there was a final sample of 35 younger adults (17 males, age range: 18-38, mean age: 22 years old) and 31 older adults (13 males, age range: 66-83, mean age: 74 years old) on the random dot motion task and a sample of 38 younger adults (15 males, age

range: 18-38, mean age: 22 years old) and 38 older adults (16 males, age range: 66-85 years old, mean age: 74 years old) on the contrast-change detection task. All recruitment and experimental procedures were approved by the School of Psychology Research Ethics Committee, Trinity College Dublin in accordance with the principles of the Declaration of Helsinki.

Procedure

Participants performed a continuous version of the random dot motion discrimination task (Kelly & O'Connell, 2013) and a contrast-change detection task (O'Connell, Dockree & Kelly, 2012). Both tasks were completed in the same session in a darkened and sound-attenuated room, with the order of the tasks pseudo-randomised across participants. In the same testing session, participants also participated in a visual oddball task, the results of which will be reported in a subsequent publication. Stimuli were presented on a 51 cm CRT monitor operating at 85 Hz and a resolution of 1024x768. Participants were seated at a distance of 55 cm from the display and were instructed to fixate a centrally-presented fixation point at all times during task performance. Prior to each task, participants carried out a practice block to familiarise themselves with the task and stimuli. During practice sessions, participants were given feedback on hits, misses and false alarms.

Random dot motion task

Participants continuously monitored a patch of incoherently moving dots for intermittent targets defined by a period of coherent motion in the leftward or rightward direction (Figure 1A). Motion direction and coherence level (30% or 60%) were varied independently and randomly on a target-by-target basis. To facilitate the measurement of motor preparation signals, participants were asked to indicate leftward motion with a left-hand button press and rightward motion with a right-hand button press. Participants were instructed to avoid guessing and to respond as soon as they were certain they perceived coherent motion. The inter-target interval, during which the incoherent motion was continuously displayed, lasted 3, 5 or 7 seconds and was randomly chosen on a target-by-target basis.

Motion stimuli were presented within an 8-degree aperture centred on the fixation point and were displayed against a black background. During incoherent motion, an average of 150 white dots (each 6 x 6 pixels) were placed randomly and independently within the circular aperture on each of a sequence of 58.8 ms frames played at 17 frames per second. During coherent motion, a proportion of the dots were randomly selected on each frame to be displaced in either a leftward or rightward direction on the following frame at a speed of 6 degrees per second. In order to accommodate very slow responses from older participants, coherent motion

targets were displayed for a maximum of 10 seconds or until 500 ms after the participant responded. Participants completed 6 blocks of the task, each lasting approximately 5 minutes and comprising 30 targets.

Gradual contrast-change detection task

Participants continuously monitored a flickering (21.25Hz) annular checkerboard pattern for intermittent targets defined by a gradual decrease in contrast. The checkerboard stimulus (inner radius=3 degrees, outer radius=8 degrees) consisted of alternating light and dark radial segments presented against a dark grey background and was located in the centre of the display. Targets consisted of a linear decrease in contrast from 70 to 40% over a period of 1.6 seconds followed by a return to 70% contrast over a further 0.8 seconds (Figure 4A). The inter-target interval, during which the stimulus flickered at 70% contrast, lasted 3, 5 or 8 seconds and was randomly chosen on a target-by-target basis. Participants were instructed to avoid guessing and to make a mouse button press with their right index finger as soon as they were certain that the annulus was decreasing in contrast. Participants completed 4 blocks of the task, each lasting approximately 4 minutes and comprising 24 targets.

EEG acquisition and preprocessing

Continuous EEG data were recorded using an ActiveTwo system (Biosemi, The Netherlands) from 64 scalp electrodes and digitised at 512 Hz. Electrodes were arranged using the standard 10/20 setup. Vertical and horizontal eye movements were recorded from four electro-occulogram (EOG) electrodes located above and below the left eye and at the left and right outer canthus, respectively. Data were analysed using custom-made scripts in MATLAB (MathWorks) drawing on EEGLAB routines for reading data files and for spherical interpolation of noisy channels (Delorme & Makeig, 2004). EEG data were re-referenced offline to the average reference and low-pass filtered to 40Hz using a two-way least-squares FIR filter.

EEG data were segmented into epochs of -750 to 2500 ms and -750 to 2100 ms for the random dot motion and gradual contrast-change detection tasks, respectively. For the gradual contrast-change detection task, epochs were baseline-corrected relative to the average signal in the 250 ms interval preceding target onset. Inspection of the data from the random dot motion task revealed that, on average, the onset of the CPP of the older group occurred before the onset of coherent motion (see Figure S2), suggesting a tendency towards premature evidence accumulation onset due to temporal uncertainty of the stimulus onset. Epochs were therefore baseline-corrected to the average signal from -600 to -500 ms with respect to coherent motion onset. Trials were rejected if the bipolar vertical EOG signal (upper minus lower) exceeded an absolute value of 200 μV or if any scalp electrode signal exceeded 100 μV within

a window of 750 ms pre-stimulus to 150 ms post-response. EEG data were converted to current source density (Kayser & Tenke, 2006) to increase spatial selectivity and to reduce the spatial blurring effect of volume conduction.

Signal analysis

SSVEP: In the contrast-change detection task the contrast-dependent steady-state visual evoked potential (SSVEP) provided a cortical representation of the sensory evidence. The SSVEP was measured at a frequency of 21.25 Hz using the discrete Fourier transform over a window of exactly 10 cycles (470 ms) of the stimulus flicker frequency in order to attenuate spectral leakage. We first identified the region of maximum amplitude of the SSVEP on the grand-average scalp topography over 10 cycles of the SSVEP immediately prior to target onset. For each participant, the pretarget SSVEP amplitude was averaged across trials and normalised by dividing by the average amplitude at 21.25 Hz across all electrodes and trials. This normalisation step was required to account for inter-individual differences in the amplitude of the SSVEP (Silberstein et al., 1990, 2001). A further baseline correction step was then applied by dividing the normalised SSVEP at each electrode by the average amplitude measured across all frequencies. On the basis of the resulting topographies, the SSVEP was averaged over 6 electrodes centred on standard sites Oz and POz for both age groups.

The temporal evolution of the SSVEP was measured for each participant by calculating the average SSVEP amplitude across trials over a 10-cycle window at the start of the epoch and progressively moving the window forward by one sample (step size= 50 ms) until the SSVEP was calculated across the entire stimulus- and response-locked epochs. The SSVEP was then normalised relative to the 470 ms pretarget window for each participant.

CPP: The timecourse of evidence accumulation was indexed by a centro-parietal positivity (CPP) in the event-related potential (O'Connell et al., 2012; Kelly & O'Connell, 2013). Stimulus-locked CPP waveforms were generated for each participant by averaging the single-trial epochs defined in *EEG acquisition and preprocessing*. Response-locked CPPs were derived by extracting epochs from -900 to 300 ms relative to the time of the response, retaining the same prestimulus baseline intervals as the stimulus-locked waveforms. For both tasks and age groups, CPP amplitude and latency were measured at a single electrode centred on the region of maximum component amplitude identified in the grand-average response-locked scalp topography (standard site Pz). The peak magnitude of the response-locked CPP was calculated as the maximum voltage within the -100 ms to 100 ms window centred on the individual response time. The buildup rate of the response-locked CPP was measured as the slope of a straight line fitted to the unfiltered ERP waveform over a time window of -250 to -100 ms.

Mu/Beta: On the random dot motion task, motor preparation signals were indexed as a decrease in lateralised oscillatory activity in the Mu and Beta bands (8-30Hz) excluding the single frequency bin at precisely 17 Hz (stimulus flicker frequency). Oscillatory power in the Mu/Beta band was measured in the hemisphere contralateral to the hand used to indicate the direction of dot motion. Mu/Beta power was measured over electrodes C3 and CP3 for right responses and C4 and CP4 for left responses with the electrode sites selected on the basis of the grand-average response-locked scalp topographies. Contralateral signals for right and left responses were averaged to produce a single contralateral waveform for each motion coherence condition. The temporal evolution of the Mu/Beta power was measured via a sliding boxcar window of 412 ms with a 58 ms step size. For each participant, Mu/Beta amplitude was normalised relative to the average signal from -600 to -500 ms with respect to coherent motion onset.

On the contrast-change detection task, lateralised Mu/Beta power was measured as the oscillatory power in the 8-30 Hz range excluding the 21.25 Hz frequency bin (stimulus flicker frequency) over the standard left hemisphere motor site C3. The temporal evolution of the Mu/Beta power was measured via a sliding boxcar window of 470 ms with a 50 ms step size. For each participant, Mu/Beta amplitude was normalised relative to the 470 ms pretarget window. The slope of the response-locked Mu/Beta power was measured over a time window of -250 to 50 ms in the response-locked waveform, while the trough of the Mu/Beta power was measured within the -100 ms to 100 ms window centred on the individual response time.

Alpha: The degree of attentional engagement during task performance was indexed by variability in pretarget alpha-band activity. For each participant, the average alpha amplitude (8-14 Hz) was calculated over the 707 ms (exactly 15 cycles of the SSVEP) interval prior to target onset across all 17 posterior electrodes. To assess the variability of alpha power between the two age groups, the coefficient of variation was calculated by dividing the standard deviation of pretarget alpha amplitude by the mean activity. The coefficient of variation is closely related to the standard deviation of a sample; however, it is not dependent on the sample mean (Barlow, 1993) and is therefore an appropriate measure for situations in which there is potentially a difference in sample means.

Bayes factor analysis: To determine the relative strength of evidence behind our approach of fixing parameters in the drift diffusion model based on our neural signals analysis, we conducted a Bayes factor analysis of the slope and amplitude measures of the CPP and Mu/Beta power for each task using JASP (JASP Team, 2017). The Bayes factor represents an alternative measure to a post-hoc power analysis that takes into account the sensitivity to distinguish between the null and alternative hypotheses. Specifically, we calculated the Jeffrey, Zellner and Siow (JZS; Rouder et al. 2009)

Bayes factor with an effect size of 1 to determine the strength of evidence in favour/against a group-level difference in the slope and peak amplitude of the neural signals of interest in each task. A JZS Bayes factor can be interpreted such that a value of three favours the null hypothesis three times more than the alternative hypothesis, while a value of one third favours the alternative three times more than the null.

Drift diffusion modelling

Behavioural data from the gradual contrast-change detection and random dot motion tasks were fit with one-choice (Ratcliff & Van Dongen, 2011) and two-choice (Ratcliff & McKoon, 2008) drift diffusion models, respectively. Drift diffusion models assume that decisions are made through a noisy accumulation process in which sensory evidence is accumulated over time from a starting point, z, and a response is initiated when the cumulative evidence reaches the correct, a, or incorrect, 0, response boundary (see Figure 2a). The rate of accumulation is called the drift rate, v, and is assumed to reflect the quality of information driving the decision process. The mean drift rate can vary across trials and this variability is assumed to be normally distributed with a standard deviation of η. There is also within-trial variability, or noise, in the evidence accumulation process. This allows that processes with the same mean drift rate terminate at different times, leading to a distribution of response times (RTs), and occasionally at the wrong boundary, leading to incorrect responses. The noise within a trial is also assumed to be normally distributed with a standard deviation of s and is fixed at 0.1 to scale the other parameters (Ratcliff & Tuerlinckx, 2002). All non-decision related processing is accounted for by a single non-decision parameter, t_{er}, that incorporates additive delays associated with sensory encoding and motor execution. For the contrast-change detection task, we assumed that the drift rate rose linearly over the duration of the target stimulus to reflect the ramping evidence signal (i.e. decreasing contrast) in this task. Given the continuous nature of the experimental tasks, we made an additional assumption that if the evidence accumulation process had not terminated at one of the response boundaries by a time deadline, the trial was classified as a miss (see also Murphy et al., 2015). The response deadlines were set to 10,000ms and 1750ms for the random dot motion and contrast-change detection tasks, respectively.

Unlike discrete versions of the random dot motion task, erroneous discriminations on the continuous version of the task were rare (~1% and 4% of targets in young and older participants, respectively). Several features of the data suggest that the few errors that did occur were likely not the result of evidence accumulation towards the incorrect decision boundary, but rather arose from erroneous action selection. First, older adults made significantly more errors when coherence was high than when it was low (5.4% vs. 2.6%, U=260, $p<0.001$, Mann-Whitney test), a pattern inconsistent

with the predictions of the diffusion model (e.g. Ratcliff & McKoon, 2008). Second, error rates were greater than false alarms rates for both younger and older adults (Younger: 0.004 vs. 0.002 per second, $p=0.01$, Older: 0.015 vs. 0.004 per second, $p<0.001$, Wilcoxon signed rank test). Given that false alarms occur in conditions with no sensory evidence (i.e. drift rate=0) and errors occur with a positive drift rate diffusing towards the correct decision boundary, if errors reflected crossings of the incorrect decision boundary we would expect to see fewer errors than false alarms. Together these observations suggest that most of the errors we observe on the motion discrimination task do not arise from the evidence accumulation process itself. As a result, errors were excluded from the diffusion modelling analysis of the motion discrimination data.

We fit a number of diffusion models to the behavioural data from each perceptual task with varying parameter constraints and estimated parameter values by minimising the G^2 statistic with a SIMPLEX minimisation routine. In order to fit the model to the data, five RT quantiles (0.1, 0.3, 0.5, 0.7, 0.9) were calculated from the RT distribution on correct trials and the proportion of trials lying between those quantiles were multiplied by the total number of trials to yield observed values. All RTs lying between 0 ms and the deadline in each task were included in these fits. These quantiles were then fed into the drift diffusion model to calculate the simulated proportion of trials that lay between these RT quantiles and were multiplied by the total number of trials to yield the model-derived expected values. The goodness-of-fit between the observed values and expected values was calculated via a G^2 test and this statistic was minimised to provide estimates of the key model parameters. In models where parameters were constrained to reflect a lack of an age group difference in our neurophysiological observations, parameters were fixed to the mean of the young and older estimates from the unconstrained model fit to the pooled data. Model comparisons were performed using Bayes Information Criterion (BIC). The BIC provides a trade-off between model complexity and goodness-of-fit, favouring a model with less parameters if the differences in the degrees of freedom outweigh the gains associated with a better model fit. The preferred model for each task was chosen based on which produced the smallest BIC value.

For each experiment, we fit the model to the data in two ways. First, we pooled data across participants and fit the model separately to the younger and older group data. Here our approach was to find the most parsimonious version of the model (fewest number of parameters) to adequately fit the data in order to avoid overfitting (see van Ravenzwaaij, Donkin & Vandekerckhove, 2017 for discussion of this topic). To this end, we first attempted to fit the pooled data with just the core components of the drift diffusion model free to vary (drift rate, decision boundary and non-decision time). However, this initial model did not provide a good fit to the data and through model simulations we identified that we also needed to include between-trial drift

rate variability as a free parameter to capture the shape of the RT distributions. The addition of between-trial drift rate variability greatly reduced G^2 values in both the younger and older data. Therefore, we fit this model to each participant's data individually and averaged the resulting parameter values across participants. These recovered parameter values were then subject to inferential statistical analyses.

Acknowledgements

This work was supported by a European Research Council (ERC) Starting Grant (to ROC) under the European Union's Horizon 2020 research and innovation program (Grant Agreement No. 638289), by a Science Foundation Ireland ERC Support Grant (to ROC) and an Irish Research Council Postgraduate Scholarship (to AH).

References

Ball, K., & Sekuler, R. (1986). Improving visual perception in older observers. *Journal of Gerontology*, *41*(2), 176-182.

Barlow JS. (1993). The Electroencephalogram: its Patterns and Origins. Cambridge, Massachusetts: MIT Press.

Bechara, A. (2005). Decision making, impulse control and loss of willpower to resist drugs: a neurocognitive perspective. *Nature Neuroscience*, *8*(11), 1458-1463.

Bennett, P. J., Sekuler, R., & Sekuler, A. B. (2007). The effects of aging on motion detection and direction identification. *Vision Research*, *47*(6), 799-809.

Betts, L. R., Taylor, C. P., Sekuler, A. B., & Bennett, P. J. (2005). Aging reduces center-surround antagonism in visual motion processing. *Neuron*, *45*(3), 361-366.

Billino, J., Bremmer, F., & Gegenfurtner, K. R. (2008). Differential aging of motion processing mechanisms: evidence against general perceptual decline. *Vision Research*, *48*(10), 1254-1261.

de Lange, F. P., Rahnev, D. A., Donner, T. H., & Lau, H. (2013). Prestimulus oscillatory activity over motor cortex reflects perceptual expectations. *Journal of Neuroscience*, *33*(4), 1400-1410.

Delorme, A., & Makeig, S. (2004). EEGLAB: an open source toolbox for analysis of single-trial EEG dynamics including independent component analysis. *Journal of Neuroscience Methods*, *134*(1), 9-21.

Di Russo, F., Pitzalis, S., Aprile, T., Spitoni, G., Patria, F., Stella, A., Spinelli, D. & Hillyard, S. A. (2007). Spatiotemporal analysis of the cortical sources of the steady-state visual evoked potential. *Human Brain Mapping*, *28*(4), 323-334.

Dockree, P.M., Barnes, J.J., Matthews, N., Dean, A.J., Abe, R., Nandam, L.S., Kelly, S.P., Bellgrove, M.A. and O'Connell, R.G. (2017). The Effects of Methylphenidate on the Neural Signatures of Sustained Attention. *Biological Psychiatry*, *82*(9), 687-694.

Donner, T. H., Siegel, M., Fries, P., & Engel, A. K. (2009). Buildup of choice-predictive activity in human motor cortex during perceptual decision making. *Current Biology*, *19*(18), 1581-1585.

Elliott, D., Whitaker, D., & MacVeigh, D. (1990). Neural contribution to spatiotemporal contrast sensitivity decline in healthy ageing eyes. *Vision Research*, *30*(4), 541-547.

Forstmann, B. U., Tittgemeyer, M., Wagenmakers, E. J., Derrfuss, J., Imperati, D., & Brown, S. (2011). The speed-accuracy tradeoff in the elderly brain: a structural model-based approach. *Journal of Neuroscience*, *31*(47), 17242-17249.

Gazzaley, A., Cooney, J. W., Rissman, J., & D'esposito, M. (2005). Top-down suppression deficit underlies working memory impairment in normal aging. *Nature Neuroscience*, *8*(10), 1298-1300.

Habak, C., & Faubert, J. (2000). Larger effect of aging on the perception of higher-order stimuli. *Vision Research*, *40*(8), 943-950.

Hanes, D. P., & Schall, J. D. (1996). Neural control of voluntary movement initiation. *Science*, *274*(5286), 427.

Hanks, T. D., Mazurek, M. E., Kiani, R., Hopp, E., & Shadlen, M. N. (2011). Elapsed decision time affects the weighting of prior probability in a perceptual decision task. *Journal of Neuroscience*, *31*(17), 6339-6352.

Hanks, T., Kiani, R., & Shadlen, M. N. (2014). A neural mechanism of speed-accuracy tradeoff in macaque area LIP. *Elife*, *3*, e02260.

Hanslmayr, S., Aslan, A., Staudigl, T., Klimesch, W., Herrmann, C. S., & Bäuml, K. H. (2007). Prestimulus oscillations predict visual perception performance between and within subjects. *Neuroimage*, *37*(4), 1465-1473.

Hauser, T. U., Fiore, V. G., Moutoussis, M., & Dolan, R. J. (2016). Computational psychiatry of ADHD: neural gain impairments across Marrian levels of analysis. *Trends in Neurosciences*, *39*(2), 63-73.

Heitz, R. P., & Schall, J. D. (2012). Neural mechanisms of speed-accuracy tradeoff. *Neuron*, *76*(3), 616-628.

Heitz, R. P., & Schall, J. D. (2013). Neural chronometry and coherency across speed–accuracy demands reveal lack of homomorphism between computational and neural mechanisms of evidence accumulation. *Philosophical Transactions of the Royal Society B: Biological Sciences*, *368*(1628), 20130071.

JASP Team. (2017). JASP (Version 0.8.3) [Computer software]. Retrieved from https://jasp-stats.org/

Kayser, J., & Tenke, C. E. (2006). Principal components analysis of Laplacian waveforms as a generic method for identifying ERP generator patterns: I. Evaluation with auditory oddball tasks. *Clinical Neurophysiology*, *117*(2), 348-368.

Kelly, S. P., & O'Connell, R. G. (2013). Internal and external influences on the rate of sensory evidence accumulation in the human brain. *Journal of Neuroscience*, *33*(50), 19434-19441.

Laming, D.R.J. (1968). Information theory of choice-reaction times. Oxford, England: Academic Press.

Lerche, V., & Voss, A. (2016). Model complexity in diffusion modeling: Benefits of making the model more parsimonious. *Frontiers in Psychology*, *7*.

Lerche, V., & Voss, A. (2017). Retest reliability of the parameters of the Ratcliff diffusion model. *Psychological Research*, *81*(3), 629-652.

Levine, B., Svoboda, E., Hay, J. F., Winocur, G., & Moscovitch, M. (2002). Aging and autobiographical memory: dissociating episodic from semantic retrieval. *Psychology and Aging*, *17*(4), 677.

Liang, Z., Yang, Y., Li, G., Zhang, J., Wang, Y., Zhou, Y., & Leventhal, A. G. (2010). Aging affects the direction selectivity of MT cells in rhesus monkeys. *Neurobiology of Aging*, *31*(5), 863-873.

Link, S. W., & Heath, R. A. (1975). A sequential theory of psychological discrimination. *Psychometrika*, *40*(1), 77-105.

Loughnane, G. M., Newman, D. P., Bellgrove, M. A., Lalor, E. C., Kelly, S. P., & O'Connell, R. G. (2016). Target selection signals influence perceptual decisions by modulating the onset and rate of evidence accumulation. *Current Biology*, *26*(4), 496-502.

Murphy, P. R., Robertson, I. H., Harty, S., & O'Connell, R. G. (2015). Neural evidence accumulation persists after choice to inform metacognitive judgments. *Elife*, *4*, e11946.

Murphy, P. R., Boonstra, E., & Nieuwenhuis, S. (2016). Global gain modulation generates time-dependent urgency during perceptual choice in humans. *Nature Communications*, *7*, 13526.

O'Connell, R. G., Dockree, P. M., Robertson, I. H., Bellgrove, M. A., Foxe, J. J., & Kelly, S. P. (2009). Uncovering the neural signature of lapsing attention: electrophysiological signals predict errors up to 20 s before they occur. *Journal of Neuroscience*, *29*(26), 8604-8611.

O'Connell, R. G., Dockree, P. M., & Kelly, S. P. (2012). A supramodal accumulation-to-bound signal that determines perceptual decisions in humans. *Nature Neuroscience*, *15*(12), 1729-1735.

Owsley, C., Sekuler, R., & Siemsen, D. (1983). Contrast sensitivity throughout adulthood. *Vision Research*, *23*(7), 689-699.

Park, D. C., & Reuter-Lorenz, P. (2009). The adaptive brain: aging and neurocognitive scaffolding. *Annual Review of Psychology*, *60*, 173-196.

Purcell, B. A., & Kiani, R. (2016). Neural mechanisms of post-error adjustments of decision policy in parietal cortex. *Neuron*, *89*(3), 658-671.

Rabbitt, P. (1979). How old and young subjects monitor and control responses for accuracy and speed. *British Journal of Psychology*, *70*(2), 305-311.

Ratcliff, R. (1978). A theory of memory retrieval. *Psychological Review*, *85*(2), 59.

Ratcliff, R., Hasegawa, Y. T., Hasegawa, R. P., Smith, P. L., & Segraves, M. A. (2007). Dual diffusion model for single-cell recording data from the superior

colliculus in a brightness-discrimination task. *Journal of Neurophysiology*, *97*(2), 1756-1774.

Ratcliff, R., Thapar, A., & McKoon, G. (2001). The effects of aging on reaction time in a signal detection task. *Psychology and Aging*, *16*(2), 323.

Ratcliff, R., & Tuerlinckx, F. (2002). Estimating parameters of the diffusion model: Approaches to dealing with contaminant reaction times and parameter variability. *Psychonomic Bulletin & Review*, *9*(3), 438-481.

Ratcliff, R., Thapar, A., & Mckoon, G. (2003). A diffusion model analysis of the effects of aging on brightness discrimination. *Attention, Perception, & Psychophysics*, *65*(4), 523-535.

Ratcliff, R., Thapar, A., & McKoon, G. (2006). Aging, practice, and perceptual tasks: a diffusion model analysis. *Psychology and Aging*, *21*(2), 353.

Ratcliff, R., Thapar, A., & McKoon, G. (2006). Aging and individual differences in rapid two-choice decisions. *Psychonomic Bulletin & Review*, *13*(4), 626-635.

Ratcliff, R., Thapar, A., & McKoon, G. (2007). Application of the diffusion model to two-choice tasks for adults 75-90 years old. *Psychology and Aging*, *22*(1), 56.

Ratcliff, R., Thapar, A., & McKoon, G. (2010). Individual differences, aging, and IQ in two-choice tasks. *Cognitive Psychology*, *60*(3), 127-157.

Ratcliff, R., Thapar, A., & McKoon, G. (2011). Effects of aging and IQ on item and associative memory. *Journal of Experimental Psychology: General*, *140*(3), 464.

Ratcliff, R., & Van Dongen, H. P. (2011). Diffusion model for one-choice reaction-time tasks and the cognitive effects of sleep deprivation. *Proceedings of the National Academy of Sciences*, *108*(27), 11285-11290.

Robertson, I. H. (2013). A noradrenergic theory of cognitive reserve: implications for Alzheimer's disease. *Neurobiology of Aging*, *34*(1), 298-308.

Roitman, J. D., & Shadlen, M. N. (2002). Response of neurons in the lateral intraparietal area during a combined visual discrimination reaction time task. *Journal of Neuroscience*, *22*(21), 9475-9489.

Rouder, J. N., Speckman, P. L., Sun, D., Morey, R. D., & Iverson, G. (2009). Bayesian t tests for accepting and rejecting the null hypothesis. *Psychonomic Bulletin & Review*, *16*(2), 225-237.

Salthouse, T. A. (1996). The processing-speed theory of adult age differences in cognition. *Psychological Review*, *103*(3), 403.

Silberstein, R. B., Schier, M. A., Pipingas, A., Ciorciari, J., Wood, S. R., & Simpson, D. G. (1990). Steady-state visually evoked potential topography associated with a visual vigilance task. *Brain Topography*, *3*(2), 337-347.

Silberstein, R. B., Nunez, P. L., Pipingas, A., Harris, P., & Danieli, F. (2001). Steady state visually evoked potential (SSVEP) topography in a graded working memory task. *International Journal of Psychophysiology*, *42*(2), 219-232.

Spaniol, J., Voss, A., & Grady, C. L. (2008). Aging and emotional memory: cognitive mechanisms underlying the positivity effect. *Psychology and Aging*, *23*(4), 859.

Starns, J. J., & Ratcliff, R. (2010). The effects of aging on the speed–accuracy compromise: Boundary optimality in the diffusion model. *Psychology and Aging*, *25*(2), 377.

Stern, Y. (2002). What is cognitive reserve? Theory and research application of the reserve concept. *Journal of the International Neuropsychological Society*, *8*(3), 448-460.

Thapar, A., Ratcliff, R., & McKoon, G. (2003). A diffusion model analysis of the effects of aging on letter discrimination. *Psychology and Aging*, *18*(3), 415.

Twomey, D. M., Murphy, P. R., Kelly, S. P., & O'Connell, R. G. (2015). The classic P300 encodes a build-to-threshold decision variable. *European Journal of Neuroscience*, *42*(1), 1636-1643.

Twomey, D. M., Kelly, S. P., & O'Connell, R. G. (2016). Abstract and effector-selective decision signals exhibit qualitatively distinct dynamics before delayed perceptual reports. *Journal of Neuroscience*, *36*(28), 7346-7352.

Wasylyshyn, C., Verhaeghen, P., & Sliwinski, M. J. (2011). Aging and Task Switching: A Meta-Analysis. *Psychology and Aging*, *26*(1), 15.

van Ravenzwaaij, D., Donkin, C., & Vandekerckhove, J. (2017). The EZ diffusion model provides a powerful test of simple empirical effects. *Psychonomic Bulletin & Review*, *24*(2), 547-556.

Yang, Y., Zhang, J., Liang, Z., Li, G., Wang, Y., Ma, Y., ... & Leventhal, A. G. (2008). Aging affects the neural representation of speed in Macaque area MT. *Cerebral Cortex*, *19*(9), 1957-1967.

Yang, Y., Liang, Z., Li, G., Wang, Y., & Zhou, Y. (2009). Aging affects response variability of V1 and MT neurons in rhesus monkeys. *Brain Research*, *1274*, 21-27.

Wagenmakers, E. J., Van Der Maas, H. L., & Grasman, R. P. (2007). An EZ-diffusion model for response time and accuracy. *Psychonomic Bulletin & Review*, *14*(1), 3-22.